Available online at www.sciencedirect.com
ScienceDirect
ELSEVIER
International Journal of Mass Spectrometry 271 (2008) 85–92
International Journal of Mass Spectrometry
www.elsevier.com/locate/ijms

Multiconfiguration Dirac–Hartree–Fock energies and transition probabilities for $2p^4(^3P)3d$–$2p^4(^3P)4f$ transitions in Ne II

Charlotte Froese Fischer[a], Yuri Ralchenko[b,*]

[a] Department of Computer Science, Box 1679B, Vanderbilt University, Nashville, TN 37235, United States
[b] Atomic Physics Division, National Institute of Standards and Technology, Gaithersburg, MD 20899-8422, United States

Received 13 August 2007; received in revised form 8 September 2007; accepted 10 September 2007

Abstract

Multiconfiguration Dirac–Hartree–Fock energies, lifetimes, and transition probabilities for transitions between $2p^4(^3P)3d$ and $2p^4(^3P)4f$ levels of Ne II are reported from calculations that included the effect of core-polarization. Transition energies are in excellent agreement with observed values. For many transitions the length and velocity gauge results agree within a fraction of a percent. Transition probabilities are compared with experimental values and the Coulomb approximation.

PACS: 31.15.Ar; 31.15.Ne; 31.30.Jv; 32.70.Cs

Keywords: Atomic structure; Multiconfiguration Dirac–Hartree–Fock method; Energy levels; Transition probabilities; Ne II

---

1. Introduction

In an article on the expanding Atomic Spectra Database (ASD) at the National Institute of Standards and Technology (NIST), Wiese [1] cites the 3p–3d transition array in Ne II as an example of an unsettled case. In spite of sophisticated calculations and a number of experimental measurements, large unresolved differences remained. Recently new measurements of branching fractions from some levels for which lifetime data were available have been reported [2]. The determination of all downward transitions in that experiment included a number of weak intersystem lines as a valuable check on theory. Closer agreement with multiconfiguration Hartree–Fock + Breit–Pauli (MCHF + BP) results [3] was found than had been the case with earlier experiments.

An equally unsettled case is the 3d–4f transition array. Because the exchange Slater integrals for $2p^4 4f$ are even smaller than for $2p^4 3d$, the LS terms are also more closely spaced and extensive term mixing occurs. Whereas the energy levels of $2p^4(^3P)3d$ span an energy range of 2582 cm^{-1} [4], those of $2p^4(^3P)4f$ span a range of only 996 cm^{-1}, and ASD levels are designated in [*jK*] notation in the absence of meaningful LSJ designations. In the present paper, energy levels, lifetimes, and transition probabilities for $2p^4(^3P)3d$–$2p^4(^3P)4f$ are reported using the multiconfiguration Dirac–Hartree–Fock (MCDHF) method, in which relativistic effects are included directly. At the same time, since both 3d and 4f are outer electrons well separated from the $2p^4$ core, a core-polarization computational model was selected. The calculated wavelengths are compared with the most recent compilation of atomic data for Ne II [5].

2. The computational procedure

The theoretical basis of our computation was the MCDHF method [6] as implemented in the GRASP2K computer code [7] and using the core-polarization model. This model has proven to be very effective for computing $2p^4(^3P)3p$–$2p^4(^3P)3d$ transitions in Ne II. In Ref. [8] theoretical results are compared for two types of calculations: MCDHF for which transition rates are reported in both length and velocity gauges, and MCHF + BP with transition rates only in the length gauge. In spite of the fact that MCHF + BP energies are in better agreement with observations, the experimental transition probabilities obtained by del

---

[*] Corresponding author. Tel.: +1 301 975 3210.
E-mail addresses: Charlotte.F.Fischer@Vanderbilt.Edu (C. Froese Fischer), yuri.ralchenko@nist.gov (Yu. Ralchenko).

1387-3806/$ – see front matter © 2007 Elsevier B.V. All rights reserved.
doi:10.1016/j.ijms.2007.09.003

Val et al. [9] for 3p–3d transitions was found to be in better agreement with MCDHF values.

The core-polarization model is expected to be appropriate also for 3d–4f transitions. The $2p^4(^3P)3d$ and $2p^4(^3P)4f$ levels have a common parent. Although there is a spin–orbit interaction between $2p^4\ ^3P_2$ and $2p^4\ ^1D_2$, the interaction is not strong. The similar interaction between $2p^4\ ^3P_0$ and $2p^4\ ^1S_0$ is even weaker. A parent changing transition would need to account correctly for the separation between the different parent energies. For the present parent preserving transitions, it is expected that MCDHF will adequately account for the spin–orbit interactions between the different parents, even though the energy separation may not be accurate.

In the MCDHF procedure, the wave function Ψ for the atomic state labeled γJ is approximated by an expansion over *jj*-coupled configuration state functions (CSFs):

$$\Psi(\gamma J) = \sum_j c_j \Phi(\gamma_j J), \tag{1}$$

where the CSFs $\Phi(\gamma J)$ are anti-symmetrized linear combinations of relativistic orbital products of the form:

$$\phi(\mathbf{r}) = \frac{1}{r} \begin{pmatrix} P_{n\kappa}(r)\chi_{\kappa m}(\hat{r}) \\ i Q_{n\kappa}(r)\chi_{-\kappa m}(\hat{r}) \end{pmatrix}. \tag{2}$$

Here κ is the relativistic angular momentum, $P_{n\kappa}(r)$ and $Q_{n\kappa}(r)$ are the large and small component radial wave functions and $\chi_{\kappa m}(\hat{r})$ is the spinor spherical harmonic. After obtaining the set of radial functions, relativistic configuration interaction (CI) calculations are carried out to determine CSF expansion coefficients by diagonalizing the Hamiltonian matrix that includes the frequency dependent Breit interaction and vacuum polarization correction. Transition probabilities between levels with separately optimized wavefunctions are computed using biorthogonal transformations [10].

In the core-polarization model, the wave function is an expansion over the set of either odd or even configuration states $2s^2 2p^4 nln'l'$ and $2s2p^5 nln'l'$, where nl and $n'l'$ are orbitals from an orbital set. In our work, the 1s,2s,2p orbitals for the parent states were determined from extended optimal level (EOL) calculations for the $^3P_{0,1,2}$ and $^1D_2$ terms of $2p^4$. These orbitals were then kept fixed for both the odd and even states. The remaining orbitals were obtained through a process that took into account the spectrum while building an orbital basis. We will refer to the {1s,2s,2p, . . . , 3s,3p,3d} set of orbitals as the $n = 3$ orbital set, {1s,2s,2p, . . . , 4s,4p,4d,4f} as $n = 4$, etc. However, for $n > 5$ the highest angular momentum for an orbital was $l = 4$, or a *g*-orbital. Calculations were done successively for $n = 3, \ldots, 7$, and each time only the new "layer" of orbitals was optimized for a selected set of atomic states.

For the even states, the $n = 3$ orbitals were optimized on all the states of $2p^4 3s$ and $2p^4(^3P)3d$, where all parents are included unless indicated otherwise. Thus, at the $n = 3$ level of the calculation, only 3p is a correlation orbital in the core-polarization expansion. The $2s2p^6\ ^2S_{1/2}$ state was omitted from the optimization. At $n = 4$, the $2p^4(^3P)4s$ and $2p^4(^3P)4d$ states were added to the optimization set with only 4p and 4f as correlation orbitals. At $n = 5$, $2p^4(^3P)5s$ and $2p^4(^1D)3d$ states were added to the optimization set, with 5p, 5d, 5f, 5g all being correlation orbitals. For $n = 6$ and 7 all orbitals were correlation orbitals, and the optimization set remained unchanged.

For the $n = 3$ odd state calculation, the orbitals were optimized on all the states of $2p^4 3p$ and omitting the $2p^5\ ^2P^o$ ground state. The 3p orbital was required to be a spectroscopic orbital with the usual nodal structure. The $n = 4$ calculation added the $2p^4(^3P)4p$ and $2p^4(^3P)4f$ states with 4p and 4f required to be spectroscopic. No new states were added to the optimization set of states for $n = 5, 6, 7$ and all orbitals were correlation orbitals of arbitrary nodal structure.

In these optimization calculations, the Dirac–Coulomb Hamiltonian was used in the variational self-consistent field procedure. Once the radial basis had been obtained, a relativistic configuration interaction (CI) calculation was performed that included the frequency dependent Breit correction, the vacuum polarization, and the QED correction. The wave functions were then used to obtain all the E1 transitions between the computed states, from which lifetimes could be determined. The *ab initio* results of all these calculations are available at http://atoms.vuse.vanderbilt.edu[11].

3. Results and evaluation of data

In this paper, we are concerned primarily with the $2p^4(^3P)3d$–$2p^4(^3P)4f$ transitions. No other theoretical data is available except for some Coulomb approximation results published in a 1966 NIST compilation [12] where LS coupling was used for determining the multiplet components. Table 1 reports the energy levels, splitting of the multiplet relative to the lowest level, difference between theoretical and observed energy levels, and lifetimes of the $2p^4(^3P)3d$ and $2p^4(^3P)4f$ levels.

Because the core-polarization model includes $2p^2 \rightarrow nln'l'$ excitations in the ground state but not in the excited states, the correlation in the present calculation is unbalanced and the energy of the ground state is too low. Consequently, the energy levels of the spectrum shown in Table 1 were adjusted so that the lowest $2p^4(^3P)3s\ ^4P_{5/2}$ agreed with the observed level. This shift, which does not affect 3d–4f transition energies, was not included at the website [11] where transitions from the ground state also are included.

The *jj*-coupling used by GRASP, identifies a state by J, parity, and an index for the eigenvalue of the computed interaction matrix. The wave function composition is distributed over many *jj*-coupled configuration states and it is customary to assign state labels by J and parity in the same order as ASD. In Breit–Pauli calculations the dominant configuration, LS term, and J are usually readily identified. This is the case for $2p^4(^3P)3d$ when accurate wave functions have been determined. A number of studies [8,13,3] have shown that the $^2F_{7/2}$ level is lower in the spectrum than $^4F_{7/2}$, whereas the earlier ASD classification, based on simpler procedures, had the levels reversed. The latest compilation [5] is now in agreement with theory. By comparison of g_J values from MCHF + BP calculations that include correlation in the $2s^2 2p^4$ core as well as core-polarization [3]

Table 1
MCDHF $2p^4(^3P)3d$ and $2p^4(^3P)4f$ energy levels (E), splitting relative to the lowest level, difference with observed (E–E_{obs}), and lifetimes in Ne II

Configuration	LS	J	E	Splitting	Differance	τ (s)
$2p^4(^3P)3d$	^4D	7/2	279484.80		347.19	2.638E−09
		5/2	279565.37	80.57	346.73	2.597E−09
		3/2	279670.52	185.71	345.65	2.476E−09
		1/2	279767.04	282.24	344.17	2.473E−09
$2p^4(^3P)3d$	^2D	5/2	280626.63		357.68	3.281E−09
		3/2	280833.31	206.67	359.76	2.844E−09
$2p^4(^3P)3d$	^4F	9/2	280510.97		337.98	2.760E−09
		7/2	281028.63	517.66	327.89	2.860E−09
		5/2	281133.41	622.43	336.17	8.641E−10
		3/2	281260.02	749.05	312.94	2.423E−09
$2p^4(^3P)3d$	^2F	7/2	280598.25	87.28	335.93	2.954E−09
		5/2	281340.80	312.17	314.87	2.436E−09
$2p^4(^3P)3d$	^4P	1/2	281078.58		310.07	2.499E−09
		3/2	281317.32	238.74	327.80	9.563E−10
		5/2	281472.77	394.19	301.41	1.189E−09
$2p^4(^3P)3d$	^2P	1/2	281670.01		337.49	4.100E−10
		3/2	282049.75	379.75	329.47	3.468E−10
$2p^4(^3P_2)4f$	$2[4]^o$	9/2	303156.93		327.88	4.233E−09
		7/2	303158.20	1.27	327.02	4.293E−09
$2p^4(^3P_2)4f$	$2[3]^o$	5/2	303171.04		326.96	4.290E−09
		7/2	303171.17	0.13	327.66	4.276E−09
$2p^4(^3P_2)4f$	$2[2]^o$	3/2	303228.45		325.89	4.298E−09
		5/2	303230.10	1.65	326.47	4.328E−09
$2p^4(^3P_2)4f$	$2[5]^o$	9/2	303259.93		324.64	4.330E−09
		11/2	303260.72	0.79	325.41	4.321E−09
$2p^4(^3P_2)4f$	$2[1]^o$	1/2	303312.90		324.04	4.364E−09
		3/2	303314.48	1.58	324.68	4.401E−09
$2p^4(^3P_1)4f$	$2[2]^o$	3/2	303825.36		316.90	4.298E−09
		5/2	303827.12	1.76	317.61	4.322E−09
$2p^4(^3P_1)4f$	$2[4]^o$	7/2	303844.70		316.19	4.318E−09
		9/2	303844.74	0.04	317.01	4.289E−09
$2p^4(^3P_1)4f$	$2[3]^o$	5/2	303915.41		314.91	4.370E−09
		7/2	303915.57	0.16	315.66	4.343E−09
$2p^4(^3P_0)4f$	$2[3]^o$	5/2	304137.93		313.26	4.333E−09
		7/2	304138.30	0.37	314.09	4.312E−09

Energies are given in cm^{-1}. Notaion A E − B means $A \times 10^{-B}$.

and from core-polarization MCDHF calculations, it has been shown that MCDHF predicts the $^4F_{3/2}$ and $^4P_{3/2}$ levels in reverse order [14] to Breit–Pauli. The wave function composition of the MCHF + BP levels agrees with ASD identifications. Though there is concern with the assignment of closely spaced levels simply in ASD order, in the absence of measured g_J values, ASD order has been selected.

The situation with regard to $2p^4(^3P)4f$ levels is somewhat different. Breit–Pauli calculations can determine the LSJ composition of $J = 11/2, 9/2, 3/2$, and 1/2 levels but not the $J = 7/2$ and 5/2 levels. For this reason, the labels were assigned in ASD order, where labels are given in jK-coupling. In Table 1 the difference of the computed and observed [15] energy levels is consistently about $330 \pm 30\,cm^{-1}$.

The lifetimes of the $2p^4(^3P)4f$ levels are remarkably uniform in spite of the considerable mixing in LSJ coupling. In the case of $2p^4(^3P)3d$ lifetimes, there is greater variation because some levels may decay to $2p^5\,^2P^o$. Table 2 compares the $2p^4(^3P)3d$ lifetimes from the present calculation with the Breit–Pauli calculation that includes the most extensive correlation [3]. Generally, the agreement is very good but some exceptions are noticed,

Table 2
Comparison of the MCDHF $2p^4(^3P)3d$ lifetimes with Breit–Pauli lifetimes [3] for calculations that included more extensive correlation

Configuration	LS	J	τ (s)	
			Present	MCHF + BP [3]
$2p^4(^3P)3d$	^4D	7/2	2.638E−09	2.578E−09
		5/2	2.597E−09	2.537E−09
		3/2	2.476E−09	2.434E−09
		1/2	2.473E−09	2.450E−09
$2p^4(^3P)3d$	^2D	5/2	3.281E−10	3.389E−10
		3/2	2.844E−10	2.973E−10
$2p^4(^3P)3d$	^4F	9/2	2.760E−09	2.743E−09
		7/2	2.954E−09	2.857E−09
		5/2	8.641E−10	9.336E−10
		3/2	2.423E−09	2.185E−09
$2p^4(^3P)3d$	^2F	7/2	2.860E−09	2.966E−09
		5/2	2.436E−09	1.809E−09
$2p^4(^3P)3d$	^4P	1/2	2.499E−09	2.401E−09
		3/2	9.563E−10	1.130E−09
		5/2	1.189E−09	1.603E−09
$2p^4(^3P)3d$	^2P	1/2	4.100E−10	5.258E−10
		3/2	3.468E−10	4.696E−10

Notation A E − B means $A \times 10^{-B}$.

Table 3
Data for the $2p^4(^3P)3d$–$2p^4(^3P)4f$ transitions in Ne II with wavelengths given in air

Multiplet terms	g_i	g_k	λ (Å)	λ_{exp} (Å)	S	f_{ik}	A_{ki} (s^{-1})
$2p^4(^3P)3d$–$2p^4(^3P_2)4f$							
^4D $^2[4]^o$	6	8	4238.46	4233.8466	1.891E+01	2.259E−01	6.291E+07
	8	8	4224.03	4219.367	3.698E+00	3.324E−02	1.243E+07
	8	10	4224.26	4219.7452	6.775E+01	6.090E−01	1.821E+08
^4D $^2[3]^o$	4	6	4255.11	4250.6469	$1.793E + 01$	3.200E−01	7.859E+07
	6	6	4236.15	4231.5332	9.960E+00	1.190E−01	4.424E+07
	6	8	4236.13	4231.6362	2.243E+01	2.680E−01	7.472E+07
	8	6	4221.74		6.795E−01	6.111E−03	3.050E+06
	8	8	4221.72	4217.1702	1.473E+01	1.325E−01	4.960E+07
^4D $^2[2]^o$	2	4	4262.20	4257.8024	1.019E+01	3.630E−01	6.664E+07
	4	4	4244.74	4240.1049	1.162E+01	2.078E−01	7.694E+07
	4	6	4244.44	4239.9190	3.642E+00	6.516E−02	1.608E+07
	6	4	4225.87	4221.086	2.177E+00	2.608E−02	1.461E+07
	6	6	4225.58	4220.8935	1.034E+01	1.238E−01	4.626E+07
	8	6	4211.24	4206.501	1.520E+00	1.371E−02	6.874E+06
^4D $^2[5]^o$	8	10	4205.96		2.475E−03	2.235E−05	6.741E+03
^4D $^2[1]^o$	2	2	4246.91	4242.210	2.428E+00	8.682E−02	3.211E+07
	2	4	4246.63	4242.038	1.004E+00	3.590E−02	6.639E+06
	4	2	4229.57	4224.641	2.082E+00	3.737E−02	2.787E+07
	4	4	4229.29	4224.473	1.498E+00	2.689E−02	1.003E+07
	6	4	4210.57	4205.596	1.210E+00	1.455E−02	8.213E+06
$2p^4(^3P)3d$–$2p^4(^3P_1)4f$							
^4D $^2[2]^o$	2	4	4156.45	4150.6893	1.108E+01	4.050E−01	7.818E+07
	4	4	4139.84	4133.868	9.732E−01	1.785E−02	6.948E+06
	4	6	4139.54	4133.691	7.929E+00	1.455E−01	3.775E+07
	6	4	4121.90		2.552E−02	3.135E−04	1.846E+05
	6	6	4121.60		6.564E−03	8.062E−05	3.166E+04
	8	6	4107.96	4101.91	1.624E−01	1.501E−03	7.909E+05
^4D $^2[4]^o$	6	8	4118.62	4112.394	1.490E+00	1.831E−02	5.401E+06
	8	8	4105.00	4098.732	2.276E−01	2.105E−03	8.332E+05
	8	10	4104.99	4098.8645	8.087E+00	7.480E−02	2.369E+07
^4D $^2[3]^o$	4	6	4124.47	4118.199	1.035E+00	1.905E−02	4.980E+06
	6	6	4106.66		6.948E−02	8.566E−04	3.388E+05
	6	8	4106.63	4100.353	2.131E+00	2.627E−02	7.793E+06
	8	6	4093.11		6.210E−02	5.761E−04	3.058E+05
	8	8	4093.09	4086.772	1.714E+00	1.590E−02	6.329E+06
$2p^4(^3P)3d$–$2p^4(^3P_0)4f$							
^4D $^2[3]^o$	4	6	4086.96	4080.510	2.792E+00	5.189E−02	1.381E+07
	6	6	4069.47		1.195E−01	1.487E−03	5.988E+05
	6	8	4069.41	4062.9730	5.349E+00	6.655E−02	2.010E+07
	8	6	4056.17		5.153E−03	4.824E−05	2.608E+04
	8	8	4056.11		1.366E−01	1.278E−03	5.183E+05
$2p^4(^3P)3d$–$2p^4(^3P_2)4f$							
^2D $^2[4]^o$	6	8	4438.09	4432.303	4.008E+01	4.572E−01	1.161E+08
^2D $^2[3]^o$	4	6	4476.61	4468.9132	1.336E+01	2.266E−01	5.027E+07
	6	6	4435.57	4428.4075	7.501E+00	8.562E−02	2.903E+07
	6	8	4435.54	4428.520	2.662E+01	3.038E−01	7.726E+07
^2D $^2[2]^o$	4	4	4465.13		8.609E−01	1.464E−02	4.898E+06
	4	6	4464.80	4457.0473	2.483E+01	4.224E−01	9.422E+07
	6	4	4424.30		2.662E−01	3.046E−03	1.557E+06
	6	6	4423.98	4416.7552	6.551E+00	7.496E−02	2.555E+07
^2D $^2[1]^o$	4	2	4448.36		1.837E−01	3.135E−03	2.114E+06
	4	4	4448.04	4439.991	7.941E+00	1.356E−01	4.571E+07
	6	4	4407.52		5.179E−01	5.949E−03	3.064E+06
$2p^4(^3P)3d$–$2p^4(^3P_1)4f$							
^2D $^2[2]^o$	4	4	4349.21	4340.020	1.461E−01	2.551E−03	8.997E+05
	4	6	4348.88	4339.8209	4.992E+00	8.716E−02	2.049E+07
	6	4	4310.46		2.002E−02	2.352E−04	1.266E+05
	6	6	4310.13		3.205E−02	3.764E−04	1.351E+05
^2D $^2[4]^o$	6	8	4306.87	4298.094	1.178E+00	1.385E−02	3.734E+06
^2D $^2[3]^o$	4	6	4332.24	4322.742	3.571E+00	6.260E−02	1.483E+07
	6	6	4293.79		3.448E−02	4.066E−04	1.471E+05

Table 3 (*Continued*)

Multiplet terms	g_i	g_k	λ (Å)	λ_{exp} (Å)	S	f_{ik}	A_{ki} (s^{-1})
	6	8	4293.77		1.421E−01	1.675E−03	4.546E+05
$2p^4(^3P)3d–2p^4(^3P_0)4f$							
^2D $^2[3]^o$	4	6	4290.87		8.366E−03	1.481E−04	3.576E+04
	6	6	4253.16		1.812E−01	2.157E−03	7.952E+05
	6	8	4253.09		2.266E−01	2.698E−03	7.461E+05
$2p^4(^3P)3d–2p^4(^3P_2)4f$							
^4F $^2[4]^o$	6	8	4540.21	4537.195	1.746E−03	1.947E−05	4.725E+03
	8	10	4518.98	4517.8334	7.749E+00	6.511E−02	1.701E+07
	8	8	4518.72		9.436E−02	7.929E−04	2.590E+05
	10	8	4415.43	4412.20	5.266E−01	3.623E−03	1.549E+06
	10	10	4415.68	4412.591	1.564E+01	1.076E−01	3.680E+07
^4F $^2[3]^o$	4	6	4563.79	4565.539	1.348E+00	2.243E−02	4.788E+06
	6	6	4537.57	4534.52	7.348E−01	8.199E−03	2.656E+06
	6	8	4537.54	4534.644	2.808E+00	3.133E−02	7.613E+06
	8	6	4516.10		9.724E−02	8.176E−04	3.565E+05
	8	8	4516.07	4514.884	4.352E+00	3.659E−02	1.197E+07
	10	8	4412.90	4409.778	9.419E−01	6.484E−03	2.776E+06
^4F $^2[2]^o$	4	4	4551.86	4553.399	3.119E+00	5.203E−02	1.675E+07
	4	6	4551.52	4553.1731	5.437E+00	9.072E−02	1.947E+07
	6	4	4525.77	4522.524	2.724E−01	3.047E−03	1.489E+06
	6	6	4525.44	4522.314	1.464E+00	1.637E−02	5.333E+06
	8	6	4504.09		4.917E−01	4.145E−03	1.817E+06
^4F $^2[5]^o$	8	10	4498.04	4496.243	1.392E+00	1.175E−02	3.098E+06
	10	10	4395.69		2.124E+00	1.468E−02	5.067E+06
	10	12	4395.53	4391.9902	1.164E+02	8.043E−01	2.314E+08
^4F $^2[1]^o$	4	2	4534.43	4535.572	1.655E+00	2.772e-02	1.799E+07
	4	4	4534.10	4535.374	4.640E+00	7.772E−02	2.522E+07
	6	4	4508.22		1.613E−01	1.812E−03	8.919E+05
$2p^4(^3P)3d–2p^4(^3P_1)4f$							
^4F $^2[2]^o$	4	4	4431.45	4431.105	1.645E+00	2.818E−02	9.573E+06
	4	6	4431.11	4430.9018	2.115E+01	3.625E−01	8.210E+07
	6	4	4406.72		1.994E−01	2.291E−03	1.180E+06
	6	6	4406.38		1.423E−01	1.635E−03	5.616E+05
^4F $^2[4]^o$	8	8	4382.76	4379.400	2.319E+00	2.009E−02	6.977E+06
	8	10	4382.75	4379.5496	8.571E+01	7.425E−01	2.063E+08
	10	8	4285.52		4.267E−03	3.024E−05	1.373E+04
	10	10	4285.51		1.874E−01	1.328E−03	4.824E+05
^4F $^2[3]^o$	4	6	4413.84	4413.113	1.254E+00	2.157E−02	4.924E+06
	6	8	4389.28	4384.223	1.634E+00	1.885E−02	4.895E+06
	6	6	4389.31	4384.1079	6.754E+00	7.790E−02	2.697E+07
	8	8	4369.19	4365.745	6.210E+00	5.397E−02	1.886E+07
	8	6	4369.21		2.391E−01	2.078E−03	9.681E+05
	10	8	4272.55	4267.382	9.295E−03	6.608E−05	3.018E+04
$2p^4(^3P)3d–2p^4(^3P_0)4f$							
^4F $^2[3]^o$	4	6	4370.91	4369.862	1.223E+01	2.125E−01	4.945E+07
	6	6	4346.85		3.269E−01	3.807E−03	1.344E+06
	6	8	4346.78	4341.514	6.828E+00	7.953E−02	2.106E+07
	8	6	4327.14		1.079E−04	9.468E−07	4.497E+02
	8	8	4327.07		1.550E−02	1.360E−04	4.846E+04
	10	8	4232.27		1.421E−02	1.020E−04	4.747E+04
$2p^4(^3P)3d–2p^4(^3P_2)4f$							
^2F $^2[4]^o$	6	8	4583.37		1.557E−02	1.720E−04	4.097E+04
	8	10	4432.76		1.057E−01	9.055E−04	2.459E+05
	8	8	4432.51	4429.640	1.247E+01	1.069E−01	3.628E+07
^2F $^2[3]^o$	6	6	4580.67	4582.043	1.326E−01	1.466E−03	4.659E+05
	6	8	4580.65		5.494E−01	6.073E−03	1.448E+06
	8	8	4429.60		5.362E+01	6.128E−01	1.562E+08
	8	6	4429.63		8.261E−01	9.442E−03	3.210E+06
^2F $^2[2]^o$	6	4	4568.66		1.560E−02	1.728E−04	8.285E+04
	6	6	4568.32	4569.604	2.950E−02	3.269E−04	1.045E+05
	8	6	4418.43		1.728E−03	1.485E−05	6.764E+03
^2F $^2[5]^o$	8	10	4412.62	4409.2987	9.445E+01	8.127E−01	2.227E+08
^4F $^2[1]^o$	6	4	4550.77	4551.67	2.749E−02	3.058E−04	1.477E+05

Table 3 (*Continued*)

Multiplet terms	g_i	g_k	λ (Å)	λ_{exp} (Å)	S	f_{ik}	A_{ki} (s^{-1})
$2p^4(^3P)3d$–$2p^4(^3P_1)4f$							
$^2F\ \ ^2[2]^o$	6	4	4447.37		3.400E−01	3.871E−03	1.958E+06
	6	6	4447.03	4446.4398	6.642E+00	7.562E−02	2.551E+07
	8	6	4304.87		1.359E−03	1.199E−05	5.754E+03
$^2F\ \ ^2[4]^o$	6	8	4443.55	4442.6865	5.662E+00	6.451E−02	1.634E+07
	8	8	4301.62		3.174E−01	2.802E−03	1.010E+06
	8	10	4301.61		1.045E+00	9.223E−03	2.660E+06
$^2F\ \ ^2[3]^o$	8	6	4429.99		9.369E−01	8.031E−03	3.639E+06
	8	8	4429.97		1.828E−01	1.566E−03	5.324E+05
	8	6	4288.57		9.126E−04	8.080E−06	3.907E+03
	8	8	4288.54		9.801E−02	8.677E−04	3.147E+05
$2p^4(^3P)3d$–$2p^4(^3P_0)4f$							
$^2F\ \ ^2[3]^o$	6	6	4386.39		4.432E−01	5.115E−03	1.773E+06
	6	8	4386.32	4385.0642	8.787E+00	1.014E−01	2.637E+07
	8	6	4248.03		1.189E−02	1.063E−04	5.237E+04
	8	8	4247.96		5.453E−05	4.874E−07	1.802E+02
$2p^4(^3P)3d$–$2p^4(^3P_2)4f$							
$^4P\ \ ^2[4]^o$	6	8	4611.26	4615.563	1.176E+00	1.291E−02	3.038E+06
$^4P\ \ ^2[3]^o$	4	6	4575.75	4574.420	1.266E+00	2.101E−02	4.462E+06
	6	6	4608.53	4612.802	3.809E−01	4.184E−03	1.314E+06
	6	8	4608.51	4612.928	1.198E+00	1.316E−02	3.100E+06
$^4P\ \ ^2[2]^o$	2	4	4514.57	4516.663	1.381E+00	4.645E−02	7.601E+06
	4	4	4563.76	4562.20	2.110E−01	3.511E−03	1.124E+06
	4	6	4563.42	4561.994	9.010E−03	1.499E−04	3.202E+04
	6	4	4596.37		1.487E−01	1.638E−03	7.756E+05
	6	6	4596.03	4600.152	1.222E+00	1.346E−02	4.249E+06
$^4P\ \ ^2[1]^o$	2	2	4497.43	4499.1166	1.233E+01	4.163E−01	1.373E+08
	2	4	4497.11		1.038E+01	3.507E−01	5.784E+07
	4	2	4546.24	4544.32	1.556E−01	2.599E−03	1.678E+06
	4	4	4545.92	4544.12	1.894E−01	3.164E−03	1.021E+06
	6	4	4578.27	4582.00	1.884E−01	2.084E−03	9.946E+05
$2p^4(^3P)3d$–$2p^4(^3P_1)4f$							
$^4P\ \ ^2[2]^o$	2	4	4396.11	4396.313	2.995E+00	1.035E−01	1.785E+07
	4	4	4442.73	4439.4610	6.853E+00	1.171E−01	3.958E+07
	4	6	4442.39	4439.2525	6.361E+00	1.087E−01	2.450E+07
	6	4	4473.63		1.410E−01	1.595E−03	7.976E+05
	6	6	4473.28	4475.390	7.794E−01	8.821E−03	2.940E+06
$^4P\ \ ^2[4]^o$	6	8	4469.77	4471.586	6.357E+00	7.200E−02	1.803E+07
$^4P\ \ ^2[3]^o$	4	6	4425.03	4421.3888	2.178E+01	3.739E−01	8.490E+07
	6	8	4455.65	4457.3507	3.255E+00	3.698E−02	9.318E+06
	6	6	4455.68	4457.0473	1.437E+00	1.633E−02	5.485E+06
$2p^4(^3P)3d$–$2p^4(^3P_0)4f$							
$^2F\ \ ^2[3]^o$	4	6	4381.88	4385.0642	1.726E+01	2.992E−01	6.929E+07
	6	6	4411.94		2.531E+00	2.904E−02	9.952E+06
	6	8	4411.86	4413.2150	4.792E+01	5.499E−01	1.413E+08
$2p^4(^3P)3d$–$2p^4(^3P_2)4f$							
$^2P\ \ ^2[3]^o$	4	6	4734.43	4732.667	2.549E+00	4.089E−02	8.112E+06
$^2P\ \ ^2[2]^o$	2	4	4638.43	4634.7623	6.444E+00	2.110E−01	3.271E+07
	4	4	4721.59	4719.608	6.905E−01	1.111E−02	3.323E+06
	4	6	4721.23	4719.363	1.705E+00	2.742E−02	5.470E+06
$^2P\ \ ^2[1]^o$	2	2	4620.33	4616.30	1.225E−01	4.027E−03	1.258E+06
	2	4	4619.99	4616.0911	1.110E+01	3.649E−01	5.702E+07
	4	2	4702.84	4700.483	2.755E−03	4.449E−05	2.683E+04
	4	4	4702.49	4700.243	1.086E+00	1.754E−02	5.292E+06
$2p^4(^3P)3d$–$2p^4(^3P_1)4f$							
$^2P\ \ ^2[2]^o$	2	4	4513.46	4508.1286	1.169E+01	3.934E−01	6.440E+07
	4	4	4592.17	4588.358	9.464E−01	1.565E−02	4.950E+06
	4	6	4591.80	4588.1330	7.739E+00	1.280E−01	2.699E+07
$^2F\ \ ^2[3]^o$	4	6	4573.26		2.078E+01	3.450E−01	7.336E+07
$2p^4(^3P)3d$–$2p^4(^3P_0)4f$							
$^2P\ \ ^2[3]^o$	4	6	4527.18	4522.7191	2.123E+01	3.561E−01	7.727E+07

The experimental wavelengths are from Ref. [5]. Notation A EB means $A \times 10^B$.

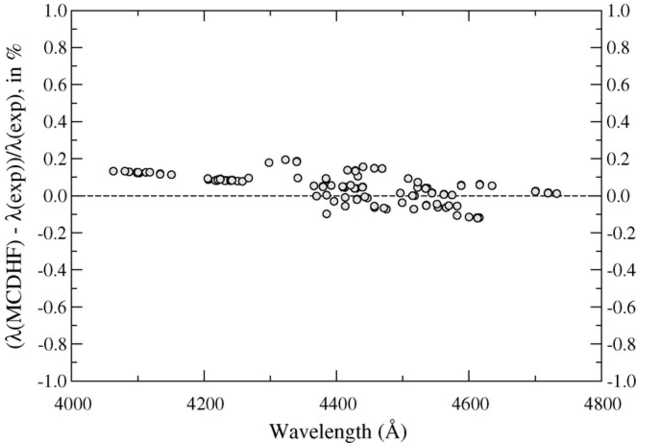

Fig. 1. Relative difference between experimental and calculated wavelengths.

such as the lifetime of ${}^2P_{3/2}$ for which the values differ by about 26%. This is a level that decays to $2p^5\,{}^2P^o$ for which the transition energy in the core-polarization model is too large compared to observations. For the $2p^4(^3P)3d$ levels the MCHF + BP lifetimes are expected to be more accurate.

Table 3 reports the calculated wavelengths, line strengths, oscillator strengths, and transition probabilities in the length gauge for all transitions within the multiplets of interest. The observed wavelengths for the $2p^4(^3P)3d$–$2p^4(^3P)4f$ transitions, as reported in the recent compilation by Kramida and Nave [5], are presented as well. The wavelengths are given in air, and the vacuum-to-air conversion of theoretical values was done using the five-parameter formula from Ref. [16]. Fig. 1 shows the relative difference between calculated and experimental wavelengths, which is seen to be less than 0.2% for all lines. The agreement in length and velocity gauges as a function of the logarithm of A_{ki} in units of $10^8\ s^{-1}$ is illustrated in Fig. 2. While large differences for very weak lines are not uncommon, the results are in near perfect agreement (less than 1.0%) for the strongest transitions over almost two orders of magnitude.

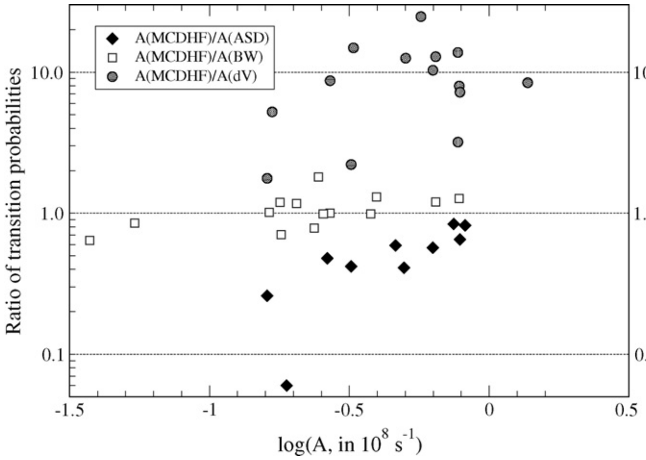

Fig. 3. Ratio of the calculated transition probabilities (present work) to other data—solid diamonds: Ref. [15]; open squares: Ref. [2]; shaded circles: Ref. [9].

Transition probabilities for quite a few 3d–4f transitions have been reported by del Val et al. [9]. Unfortunately, their line identifications were based on the 1968 compilation by Striganov and Sventitskii [17] which, as follows from Ref. [5], is incorrect for most of the 3d–4f transitions. Even for those lines that are identified correctly, the difference between the measured and presently calculated transition probabilities is generally very large. In Fig. 3 the ratios of present values to the experimental results are plotted as a function of the logarithm of the A_{ki} value, in units of $10^8\ s^{-1}$. One can see that the typical difference between our calculations and Ref. [9] is about a factor of 5–10. On the other hand, agreement with the newest measurements [2] is very good, mostly within 25%. Note that the authors of Ref. [2] used experimental wavelengths to derive transition probabilities from theoretical oscillator strengths. Therefore there is a few-percent difference between our present *A*-values and our results as cited in Ref. [2]. Finally, the Coulomb approximation results from the NIST Atomic Spectra Database [15] are seen to be consistently smaller than the present calculations, yet the difference is mostly within 50%.

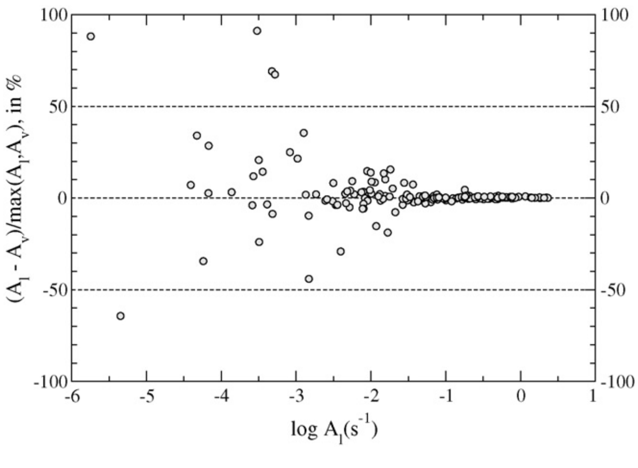

Fig. 2. Relative difference between the length and velocity gauge results for transition energies.

Acknowledgments

This paper is dedicated to the memory of Yong-Ki Kim whose doctoral thesis, under the direction of Clemens C. J. Roothaan, was entitled Relativistic self-consistent-field theory for closed shell atoms. It remained a topic of interest throughout his career.

The present work was supported in part by the Chemical Sciences, Geosciences and Biosciences Division, Office of Basic Energy Sciences, Office of Science, U.S. Department of Energy (C.F.F.) and Office of Fusion Energy Sciences, U.S. Department of Energy (Yu.R.).

References

[1] W. Wiese, Phys. Scr. T105 (2003) 85.
[2] M. Bridges, W. Wiese, Phys. Rev. A 76 (2007) 022513.
[3] C. Froese Fischer, G. Tachiev, Atomic Data Nucl. Data Tables 87 (2004) 1.
[4] The customary unit cm^{-1} used here is related to the SI units of energy (Joules) by $1\ cm^{-1}$=$1.98644561(34)\times10^{-21}$ J. See P.J. Mohr, B.N. Taylor, The 2002 CODATA Recommended Values of the Fundamental Physical Constants Web Version 4.0, Available at http://physics.nist.gov/constants.

[5] A.E. Kramida, G. Nave, Eur. J. Phys. D 39 (2006) 331.
[6] I.P. Grant, Relativistic Quantum Theory of Atoms and Molecules, Springer Series on Atomic, Optical, and Plasma Physics, Springer, New York, 2007.
[7] P. Jönsson, C. Froese Fischer, X. He, I.P. Grant, Comput. Phys. Commun, 177 (2007) 597.
[8] C. Froese Fischer, X. He, Can. J. Phys. 77 (1999) 177.
[9] J.A. del Val, J.A. Aparicio, V.R. González, S. Mar, J. Phys. B 34 (2001) 2513.
[10] J. Olsen, M. Godefroid, P. Jönsson, P.Å. Malmqvist, C. Froese Fischer, Phys. Rev. E 52 (1995) 4499.
[11] G. Tachiev, C. Froese Fischer, http://atoms.vuse.vanderbilt.edu.
[12] W.L. Wiese, M.W. Smith, B.M. Glennon, Atomic Transition Probabilities, vol. I, NSRSD-NBS-4, U.S. Government Printing Office, Washington, DC, 1966.
[13] M.R. Godefroid, A. Hibbert, Mol. Phys. 98 (2000) 1099.
[14] C. Froese Fischer, P. Jönsson, J. Mol. Struct. (Theochem.) 537 (2001) 55.
[15] Yu. Ralchenko, F.-C. Jou, D.E. Kelleher, A.E. Kramida, A. Musgrove, J. Reader, W.L. Wiese, K. Olsen, NIST Atomic Spectra Database (Version 3.1.2) (Online). Available at http://physics.nist.gov/asd3 (June 22, 2007), National Institute of Standards and Technology, Gaithersburg, MD, 2007.
[16] E.R. Peck, K. Reeder, J. Opt. Soc. Am. 62 (1972) 958.
[17] A.R. Striganov, N.S. Sventitskii, Tables of Spectral Lines of Neutral and Ionized Atoms, Plenum, New York, 1968.